ISSN 1063-780X, Plasma Physics Reports, 2024, Vol. 50, No. 4, pp. 514–523. © The Author(s), 2024. This article is an open access publication.

TOKAMAKS

Study of the Method of Photon Neutralization of Powerful Beams of Negative Ions at the Budker Institute of Nuclear Physics

S. S. Popov[a,b,*], M. G. Atlukhanov[a,b], A. V. Burdakov[a,c], A. A. Ivanov[a], V. V. Kurkuchekov[a,b], A. L. Sanin[a,b], D. I. Skovorodin[a,b], Yu. A. Trunev[a,b], and I. V. Shikhovtsev[a,b]

[a] *Budker Institute of Nuclear Physics, Siberian Branch, Russian Academy of Sciences, Novosibirsk, 630090 Russia*

[b] *Novosibirsk State University, Novosibirsk, 630090 Russia*

[c] *Novosibirsk State Technical University, Novosibirsk, 630073 Russia*

**e-mail: s.s.popov@inp.nsk.su*

Received November 30, 2023; revised February 6, 2024; accepted February 10, 2024

Abstract—A short review of the studies carried out at the Budker Institute of Nuclear Physics, Siberian Branch, Russian Academy of Sciences (BINP SB RAS) on the photon neutralization of the beams of negative ions is presented. The principal distinctive feature of the presented approach consists in the nonresonant accumulation of photons in a limited space. Their confinement is based on the adiabatic motion of photons in a system of concave mirrors, which is insensitive to the quality of the injected radiation. An analysis is carried out of the possibility of using the neutralizer based on such a nonresonant photon trap in large-scale installations such as ITER and TRT, and a future experiment is described on the photon neutralization using a beam of negative hydrogen ions with energy up to 130 keV and a current of about 10 mA.

Keywords: photoneutralization, nonresonant photon trap, adiabatic invariants, optical fiber laser, ITER, TRT

DOI: 10.1134/S1063780X24600233

1. INTRODUCTION

The traditional approach to the neutralization of beams of negative ions for such applications as the heating of the plasma and its diagnostics by neutral beams is to use a gas or a plasma target to detach excess electrons. However, both of these approaches have limited efficiency. For example, in the systems of neutral injection with the energy of atoms of 1 MeV that are currently being designed [1], the efficiencies of neutralization for the gas and plasma targets are 60 and 85%, respectively, which substantially affects the total efficiency of the designed nuclear reactors. These approaches also introduce other drawbacks that are significant for some applications, such as the worsening of the vacuum conditions due to the gas puffing, the appearance of admixtures in the beam, and the strengthening of the breakdown phenomena in the accelerator. The conversion target that is devoid of these drawbacks and can be used to transform the beam of negative hydrogen ions into the beam of atoms is the photon target (see Fig. 1).

If the photon energy exceeds the electron affinity energy of the hydrogen atom (0.754 eV) but is lower than its ionization energy (13.6 eV), the main interaction between the beam and the target is the photodetachment of the electrons from the negative ions. This makes it possible for the atomic yield from such a target to be close to unity, since the reverse process has a low probability, and total photoneutralization is impossible.

The neutral current density at the exit from the trap is

$$j(s) = j_{-}(0)\left(1 - \exp\left(-\frac{\sigma c}{V\hbar\omega}\int_0^s W dz\right)\right), \qquad (1)$$

where j and j_{-} are the densities of the neutral current and negative ion current, W is the radiant energy density, σ is the photodetachment cross section, V is the electron speed, z is the coordinate along the beam, and s is the beam path inside the target.

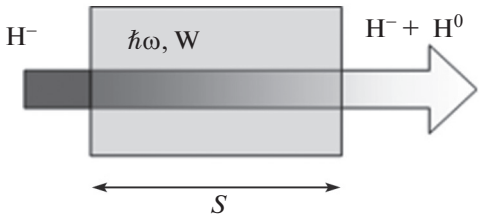

Fig. 1. Photodetachment cross section.

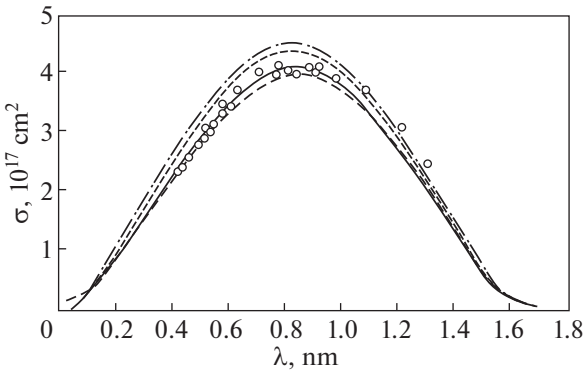

Fig. 2. Schematic diagram of a photon neutralizer.

The cross section of the electron photodetachment from a negative hydrogen atom, depending on the wavelength, is shown in Fig. 2 [3–5]. Theoretically, the photodetachment cross section was calculated in [5]. The estimates showed that, taking into account the decrease in photon energy with increasing wavelength, the energy cost of a single act of photoneutralization is minimum at the radiation wavelength of 1 μm.

This determines, to a substantial degree, the choice of the radiation source for the photoneutralizer. For a neutralizer with a length of about 1 m, the required energy density is $W \sim 10^{-5}$ J/cm^3, or alternately, its intensity is $I \sim Wc \sim 3 \times 10^5$ W/cm^2. This requires, on the one hand, high pumping power and on the other, highly efficient photon accumulation. Despite the obvious technical difficulties, the problem of the photon neutralizer needs to be solved because the construction of economically viable thermonuclear energy plants appears impossible without increasing the efficiency of the neutralization of the beams of negative ions by means of photon neutralization.

2. POSSIBLE OPTICAL SCHEMES OF THE PHOTON ACCUMULATOR

To date, many possible schemes of photon neutralizers were proposed. Starting from the first work [7], they usually include an optical resonator, inside of which the beam of negative ions is stripped, and a powerful laser pumping system. With few exceptions, these are solid-state laser systems (see, e.g., [8–10] and the references therein) with extreme flows of radiant energy on the resonator wall. Despite some substantial differences between the optical schemes proposed in these works, all of them are based on accumulating the photons in the Fabry–Pérot resonator, whose simple scheme is shown in Fig. 3. Such schemes have a number of substantial limitations.

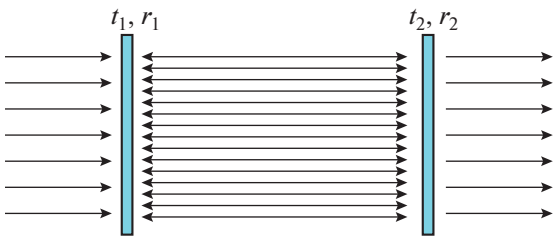

Fig. 3. Schematic diagram of the standard Fabry–Pérot resonator.

Indeed, the rate of radiation accumulation in this scheme is

$$I/I_0 = \zeta = \frac{t_1^2\left(r_2^2+1\right)}{1-2r_1r_2\cos(\delta)+\left(r_1r_2\right)^2}, \qquad (2)$$

where I_0 and I are the injected and accumulated radiation intensities, respectively; t_1, t_2, r_1, and r_2 are the amplitude transmission and reflection coefficients from the input and output mirrors; and δ is the phase shiftover two passages between the mirrors. Taking into account the losses (2), we have

$$\zeta \approx \frac{t_1^2\left(r_2^2+1\right)}{1-2r_1r_2\sqrt{(1-A)}\cos(\delta)+\left(r_1r_2\right)^2(1-A)}, \qquad (3)$$

where A is the total dissipative radiation loss over the two passages. In the resonance, at $r_2^2 \approx 1$, the radiation amplification is

$$\zeta = \frac{2t_1^2}{\left(1-r_1\sqrt{1-A}\right)^2} \approx \frac{8t_1^2}{\left(1-r_1^2+A\right)^2}. \qquad (4)$$

Modern technology allows one to produce mirrors with reflectivity higher than 0.999, which leads to radiation accumulation of several thousand times. Thus, in [10], the reflectivity was set at 0.9996. However, apart from effective reflection, such concepts pose very exacting requirements on the quality of the incoming laser radiation to satisfy the resonance conditions over a large number of passages. The resonance frequency detuning in Eq. (3), determined by the resonator length L, its instability ΔL, and the spectral line width $\Delta\lambda$ during the effective photon accumulation is limited by

$$1-\cos(\delta) \approx \left|\frac{4\pi\Delta L}{\lambda}\right| + \left|\frac{4\pi L\Delta\lambda}{\lambda^2}\right| \ll 1-r_1r_2\sqrt{1-A} \approx 5\times10^{-4}. \qquad (5)$$

For the parameters of the injectors similar to those developed for ITER or DEMO [1], when the resonator length is set as no shorter than 100 m [11], the width of the radiation line has to be less than

$\nu \sim \frac{\Delta\lambda}{\lambda^2} c \approx \frac{1 - r_1 r_2}{4\pi L} c \sim 100$ Hz. Otherwise, the "resonant" smallness of the denominator will not be true for the entire pumping spectrum. Today, the development of a powerful (1 kW) radiation source with such a thin line is a very complicated problem [11]. Additionally, due to the strict resonance conditions, the problem of spatial and temperature stabilization is no less technically challenging [12].

The development of a photon target based on modern technology appears possible and requires the revision of the resonator design (mirrors and radiation windows) and the development of a stationary radiating system with sufficient power and economic efficiency. The present state of research concerning this problem can be found in the review [13].

An alternative resonance accumulator could be a system of mirror surfaces that provides multiple reflections of rays and their adiabatic confinement in a certain region. Similarly to the resonant photon accumulators, the integral radiation energy accumulation in such a system will be determined by the losses to reflection and the time during which the rays escape outside the system. The principal difference from the resonant accumulators here is the absence of the strictly specified condition for the phase ratios between the large number of rays inside the trap. In this case, we have a system of the type of mathematical billiards with open regions that is not sensitive to the frequency and spatial spectrum of the input radiation. The latter substantially simplifies the research and development of the radiation source with sufficient power. We can in developing use a system of powerful industrial fiber-laser [14] or diode lasers.

This approach to radiation accumulation was proposed and experimentally tested at BINP SB RAS [15, 16]. Later, the photon neutralization of the beams of neutral hydrogen and deuterium ions was demonstrated experimentally with a record degree of neutralization that exceeded 95% [17]. The particle energy was up to 12 keV. The width of the neutralization region in the experiment was about 2 mm. The efficiency of the radiation accumulation was about 400. The mirrors were constructed from smoothly paired cylindrical and spherical segments.

3. SCHEME OF THE NONRESONANT PHOTON NEUTRALIZATION IN LARGE-SCALE DEVICES AND ITS EFFECT ON THE TOTAL EFFICIENCY OF THE ATOMIC INJECTOR

The principle scheme of the neutralizer in a geometry close to that of the ion beams at ITER is shown in Fig. 4 [18]. Each mirror consists of a cylindrical central part that is smoothly paired with spherical tips. The length of such an accumulator can reach 10 m, which is caused by the necessity to remove the radiant heat load and the conditions of the longitudinal confinement at the substantial distance of 6 m between the mirrors. For the system of neutral injection similar to the one accepted at TRT [19], the energy, parameters, and scale of the photon accumulator remain nearly as impressive (see Table 1). The results of the numerical simulations of the illumination in the accumulator and the achievable neutralization profile are shown in Fig. 5.

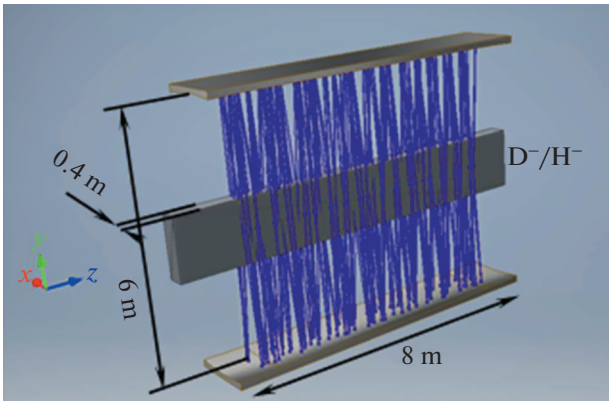

Fig. 4. Schematic diagram of the nonresonant photon neutralizer for ITER.

Let us estimate the efficiency of injection in the proposed neutralization concept. The neutralization degree we will write as (1)

$$K(P) = 1 - \exp\left(\frac{-\sigma P}{E_0 d V}\right), \tag{6}$$

where d is the width of the neutralization region, E_0 is the photon energy, and V is the ion speed. The integral radiation power P inside the trap is equal to $= P_0/\left(1 - r^2\right)$, where P_0 is the power of the optical pumping in the trap and r is the amplitude reflection coefficient. Consequently, the efficiency of the neutral injection system with a flow of negative ions with power P_- (at total energy consumption for the accelerator and the accompanying systems P_{ac}) by a laser with efficiency η_l is determined by the expression

$$\eta(P_0) = \frac{K(P_0) P_-}{P_{ac} + P_0/\eta_l}. \tag{7}$$

If we use the estimate of P_{ac} about 67 MW done in [6], we obtain the estimated dependence of the efficiency of the atomic injector on the power of photons pumping into the trap shown in Fig. 6. In the same figure, the degree of neutralization is also shown. Since Eq. (6) does not account for the losses on the cooling of the mirrors and other elements of the laser system and their amortization, it is reasonable to estimate the optimum pumping level at about 300 kW. The further increase in the efficiency is negligible.

Table 1. Parameters of ion neutralizers at ITER and at TRT

	ITER	TRT
Beam power, H^-/D^-, MW	40	5
Beam particles energy, MW	<1	<0.5
Mirror reflectivity	0.9995	0.9995
Neutralization region cross section, cm^2	40 × 100	20 × 20
Accumulator length, m	8	2
Intermirror distance, m	6	1
Laser injection power, kW	300	150
Wavelength, μm	1.07	1.07
Neutralization degree, H^-/D^-, %	>90/>95	>90/>95
Injection efficiency, %	>50%	–

When the traditional gas neutralizer is used, the injection efficiency is limited by a value of 26% [6] at the equivalent atomic current at the output of 17 A compared to 36 A during photon neutralization. Note that the transverse profile of the neutralized beam plays an important role. It is seen in the neutralization profile (Fig. 5b) and Eq. (6) that the transverse size d of the beam has to be as compact as possible.

4. STATUS OF THE EXPERIMENT ON NEUTRALIZING THE BEAMS OF NEUTRAL IONS IN THE STATIONARY REGIME

The first experimental demonstration of adiabatic confinement was given in [15]. In the work, a simple scheme of nonresonant accumulation based on a spherical mirror was used. The accumulation efficiency was determined by the photometry of the radiation dissipated on the mirror surface (see Fig. 7).

As a result, the accumulation efficiency exceeded 300 at about 1000 reflections with significant contribution that constituted about 99% of the accumulated power. This experiment was used to develop an accumulator with a mirror shape similar to Fig. 4 that is applicable for the photoneutralization of the beams of negative ions. The mirrors were assembled from separate segments of cylindrical and spherical shapes (see Fig. 8).

The radiation accumulation in the trap made from a pair of such mirrors was studied in [16]. The accumulation efficiency determined by direct registration of the dependence of the radiation lifetime on the absorbers that were introduced was about 430. The accumulator was used in the experiment on the neutralization of H^- and D^- beams [17], whose scheme is shown in Fig. 9.

The optical radiation from the laser collimator *1* was sent through the light divider *2* and then focused by the lens *3* onto the entrance aperture of the optical accumulator *4*. The angular spread of the system was

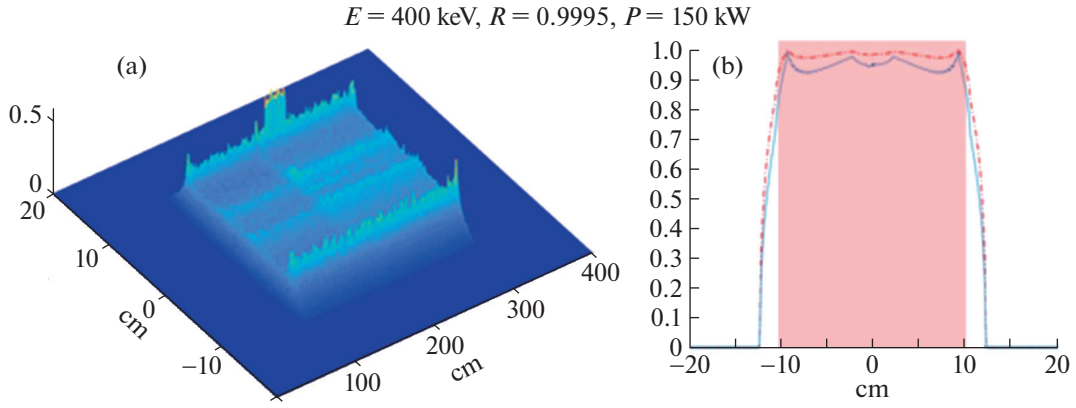

Fig. 5. Numerical simulations of the photon neutralizer for the system of neutral injection similar to the system at TRT: (a) laser radiation intensity distribution in the center of the photon accumulator and (b) transverse profile of the neutralization (the solid line is for the H^- beam, the dashed line is for the D^- beam, and the rectangular background is the transverse size of the beam).

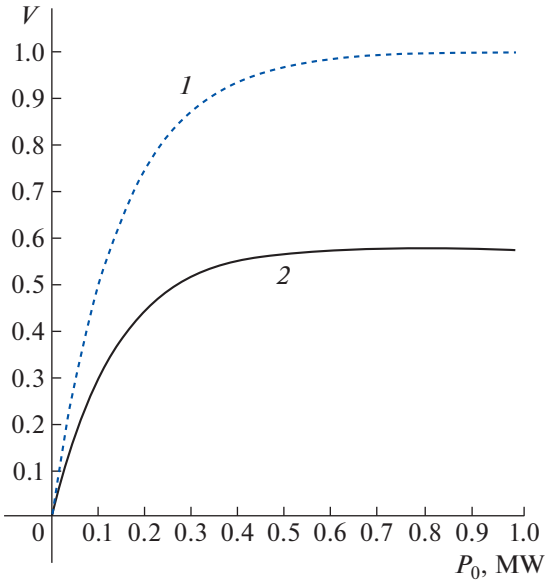

Fig. 6. (*1*) Dependence of the ionization degree on the pumping power of photons into the target and (*2*) efficiency of the ITER injector at the power of the negative ion beam equal to 40 MW.

about 3°. The photon trap itself was located in the vacuum chamber *5*. The light divider *2* directed a small fraction of the injected radiation onto gauge *6*. The camera *7* allowed us to use the divider to control the targeting of the focal spot on the entrance aperture. The distance between the mirrors was 50 mm. The H^+ and D^+ ion beams with particle energies ranging from 6 to 12 keV were generated by the DINA 4A source [20]. The gas target at the exit nozzle of the source generated the negative ion fraction. The rotating magnet *9* separated this fraction from the neutral and positive components and directed it to the chamber *5* and neutralizer *4*. The diaphragms *10* formed the beam cross section that was coupled to the neutralization region in the photon trap. The beam composition after the neutralizer was determined by the magnetic analyzer *11*. In the experiment with this scheme, a record to-date neutralization degree was achieved, as is shown in Fig. 10. Here, lines *1* and *3* are the time dependences of the negative ion current without photon trap pumping and with the pumping, respectively. The time dependence *2* is the monitor of the laser pumping. In panel (b) of this figure, the time dependences cleared from noise and displacement are shown. Signal *3* is scaled vertically relative to signal *1* for better agreement. The difference of units and the inverse scaling coefficient provide a neutralization degree of about 98%. The obtained results are substantially ahead of the progress achieved in the resonant approach (see review [13]).

During the transition from small-size photon neutralizers (such as described in [17]) to the scale required for ITER and TRT, a number of difficulties arise. They stem from the need to produce mirrors or their elements with a substantially larger area and with a better reflectivity. Additionally, the question also appears of the cost of such production and the longevity of the mirror surface under the conditions of the thermonuclear experiments and the associated flows of high-energy particles. It is practical to solve these problems step-by-step, by increasing the mirror size and the accumulated power, refining the production technology and control of their lifetime, and at the same time work over the auxiliary systems (adjustment, cooling, etc.). The next such step is the implementation of the photon neutralization of a beam of negative hydrogen ions with energies up to 130 keV, current up to 14 mA and duration up to the continuous operation mode. The scheme of the prepared experiments is shown in Fig. 11. The ion source is the injector for the tandem ion accelerator developed at BINP SO RAS [21]. Its main parts are the source *1* of negative ions with cesium surface–plasma generation and the accelerating tube *2* separated by the rotating magnet. The latter allows one to effectively separate the negative ions from the electron component in the extracted flow. In the continuous operation regime, the injector can consistently produce a beam with a current up to 14 mA. The energy range can vary from 25 to 130 keV. The vacuum chamber of the photon neutralizer *3* will be the same as the one used in [17].

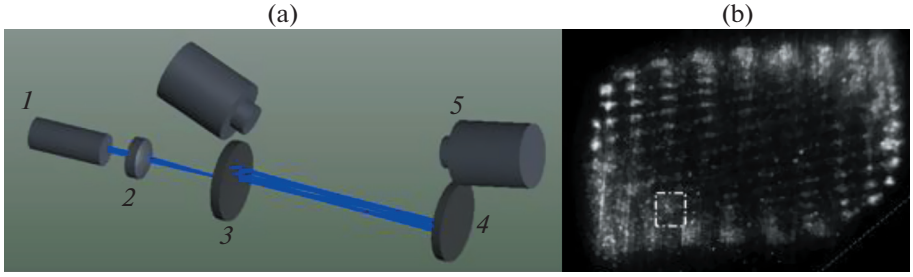

Fig. 7. (a) Scheme of the experiment: (*1*) radiation source, (*2*) lens, (*3*) mirror with input slit, (*4*) blind mirror, and (*5*) photocameras and (b) photometric profile of the intensity of the accumulated radiation at mirror *4*; the square marks the region of the first incidence of the light beam on the mirror.

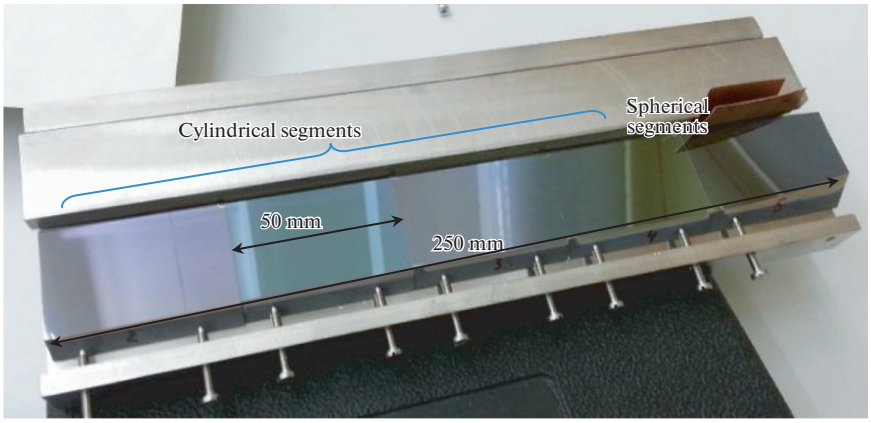

Fig. 8. Possible scheme of the assembly of the photon accumulator mirror from cylindrical and spherical segments.

To limit the transverse size of the beam at the entrance of the neutralizer, a system of two adjustable diaphragms *4* is installed. In addition to coupling the beam cross section with the neutralization region, the diaphragms will protect the mirrors from the particles exiting from the tube at large angles or scattered at large angles on their way to the neutralizer *5*. For the discussed experiment, mirrors with a complicated shape of the reflective surface were produced. The technical drawing of the mirror mount is shown in Fig. 12. The 400-mm-long cylindrical part of the mirror smoothly transitions into its toroidal part. The radius of the cylinder and the minor radius of the torus are of 300 mm and the major radius of the torus is of 1000 mm. The transverse size of the light-reflecting surface is about 100 mm and its longitudinal size is 500 mm; the entrance aperture also has a complicated shape for the input of the converging light beam and a sufficiently effective heat removal from the vicinity of the narrow neck whose diameter is 0.5 mm. Monocrystalline silica was chosen as the mount material because it has a number of advantages compared to the traditional quartz: a high heat conductivity, which simplifies heat removal, a high electrical conductivity needed to extract the charge and voltage from the dielectric coating, and an acceptable producibility during polishing and buffing.

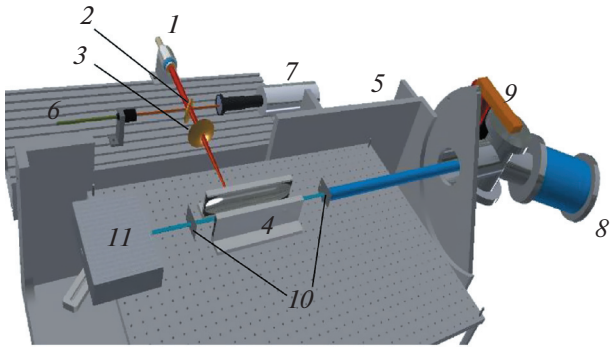

Fig. 9. Scheme of the experiment on the neutralization of H^- and D^- beams taken from [17]: (*1*) laser collimator, (*2*) light divider, (*3*) lens, (*4*) photon accumulator, (*5*) vacuum chamber, (*6*) gauge of the pumping radiation, (*7*) photocamera that controls the entrance of the radiation in the input aperture, (*8*) generator of beams of positive ions, (*9*) rotating magnet, (*10*) forming diaphragms, and (*11*) magnetic analyzer.

The effect of the particle flows on the lifetime of the accumulator mirrors with a multilayer dielectric coating and, consequently, the optimization of the diaphragms with the mirror positions warrants a separate study. To date, in the developed project, the distance between the mirrors is chosen to be about 10 cm. On the one hand, this allows one to create a neutralization region with a width of about 1 cm (see Fig. 13) that is efficiently filled with rays, and on the other, to relatively securely prevent the bombardment of the mirror surface by the high-energy particles. After the neutralizer, the beam passes through a unit with ports for the optical probing and thence into the magnetic analyzer of its charge composition.

5. THE EFFICIENCY OF ACCUMLATION OF THE RADIANT ENERGY

The simulation results of the accumulator using such mirrors are shown in Fig. 13. To the difference from the large-scale schemes of the ITER type [18], here, only one injection point is designed leading to less homogeneous illumination and neutralization profiles an also to more diffuse boundaries (see Fig. 5a). The separate intensity peaks are connected to the location of the radiation input point and the average sharpness of the transverse profile is caused by the compaction of rays near the turning points during their adiabatic motion. At a relatively powerful pumping (4 kW) of the accumulator, the average neutralization over the width of 10 mm can be up to 80%. The

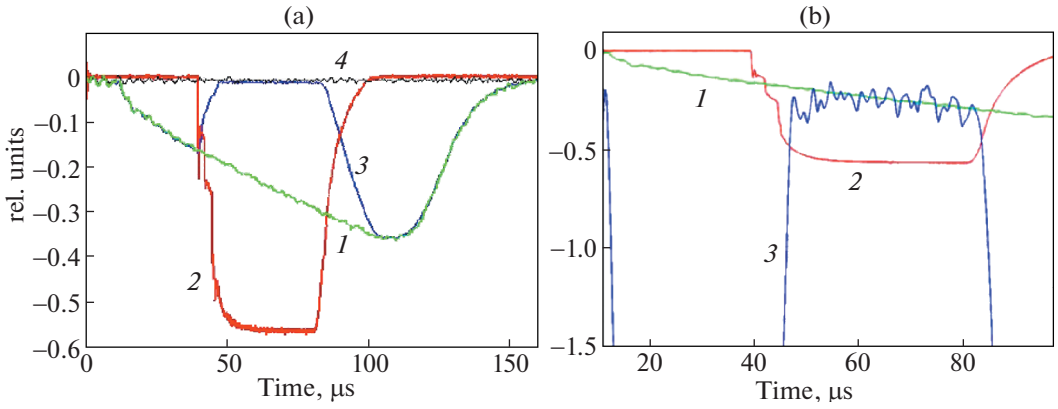

Fig. 10. (a) Time dependences in the experiments on the neutralization of the D^- beam with particle energy of 6.5 keV and (b) the same after filtering the noise and scaling: (*1*) negative ion beam without neutralization, (*2*) laser pumping monitor, (*3*) negative ion beam affected by the neutralizer, and (*4*) noise and displacement of the zero line (plate (a) only).

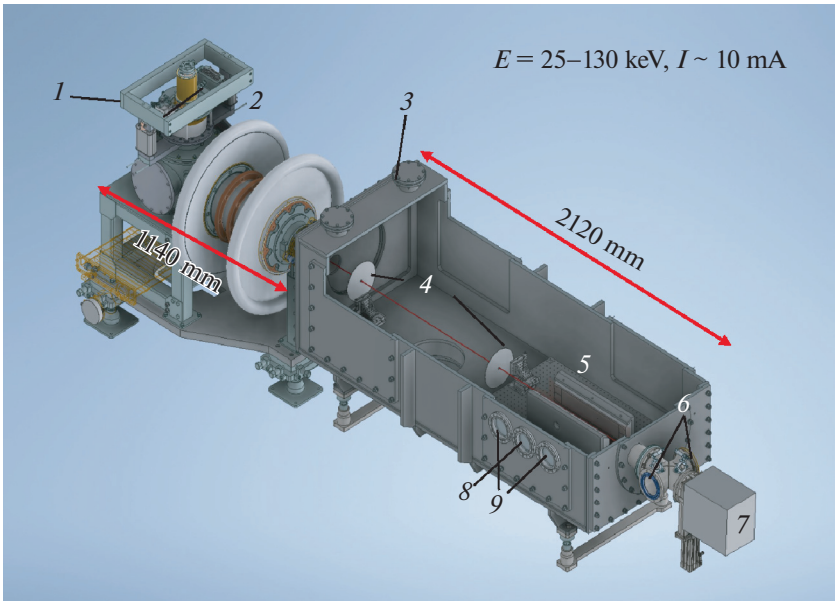

Fig. 11. Model of the experimental device neutralizing the beam of negative hydrogen ions: (*1*) ion source, (*2*) accelerating tube, (*3*) vacuum chamber of the neutralizer, (*4*) forming diaphragms, (*5*) photon accumulator, (*6*) ports of the optical diagnostics of the neutralized beam, (*7*) magnetic beam analyzer, (*8*) port for the input of laser radiation into the chamber, and (*9*) auxiliary ports of the system inputting the radiation into the photon accumulator.

existing optical fiber laser produced by IPG guarantees the required power. The quality of the laser beam allows one to introduce the radiation through the hole in mirror with the necessary focusing angle. Currently, the mirrors are produced by Research Institute Scientific Production Association "LUCH." The accumulator assembled from them (see Fig. 14) is studied with regards to the efficiency of containment of the radiant energy. According to the first results, the accumulation coefficient is about 2000. This agrees with the surface reflectivity of 0.9995 prescribed by the design specification. The studies (which will be reported in detail later) are carried out by the scheme and mathematical model close to [16]. The preliminary results show the technical feasibility of producing such complicated mirrors.

6. MAIN STAGES OF THE EXPERIMENTAL PROGRAM OF THE NEUTRAL ION BEAM NEUTRALIZATION

The following main stages are outlined in the experimental program:

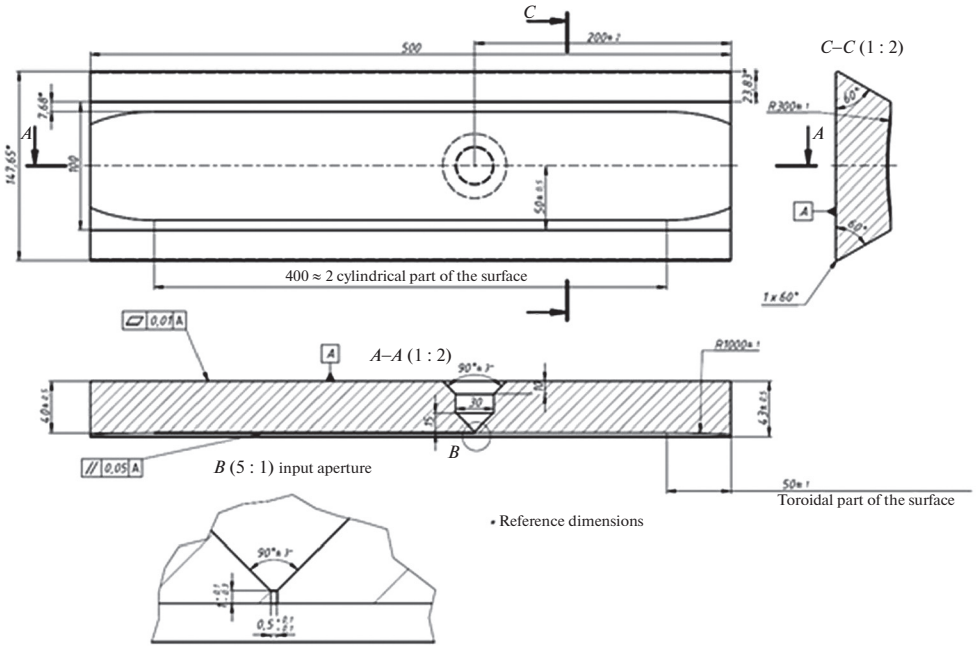

Fig. 12. Technical drawing of the mount of the mirror of the photon accumulator.

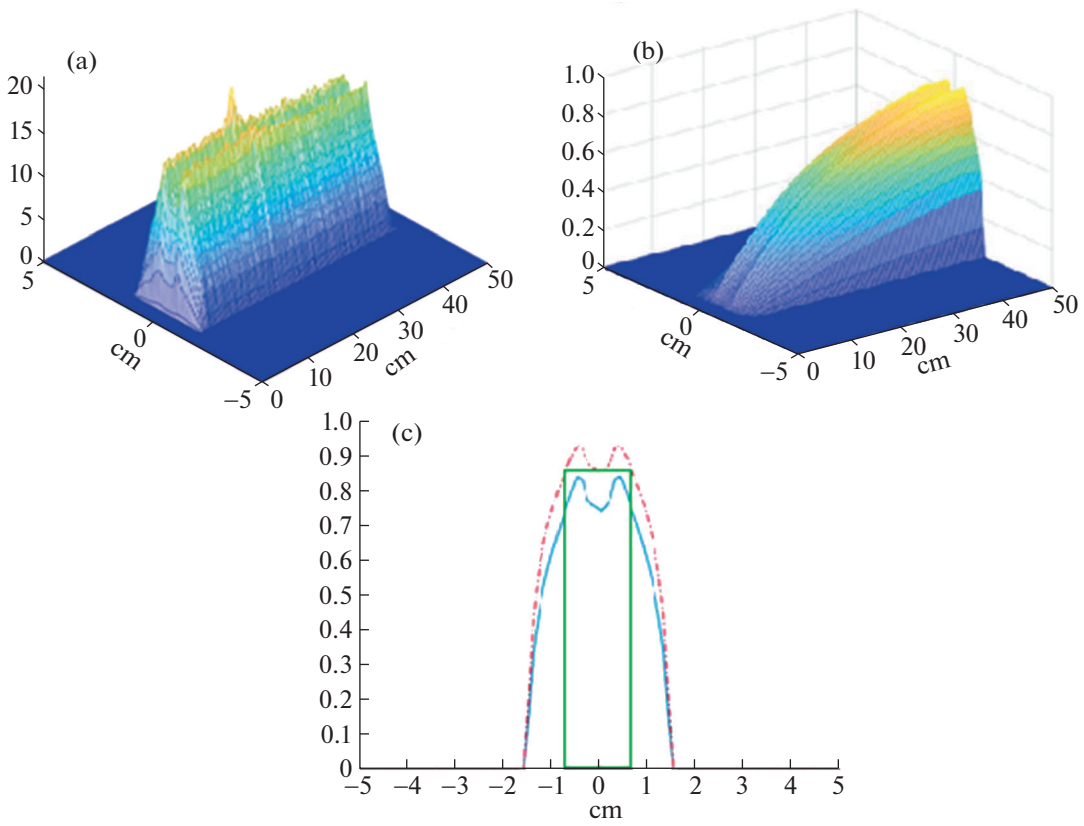

Fig. 13. Numerical simulation of the neutralization experiment: (a) distribution of illumination in the neutralization region; (b) dependence of the neutralization degree on the coordinates in the neutralization region, and (c) final neutralization profile, where the solid line corresponds to the hydrogen beam and the dashed line to the deuterium beam.

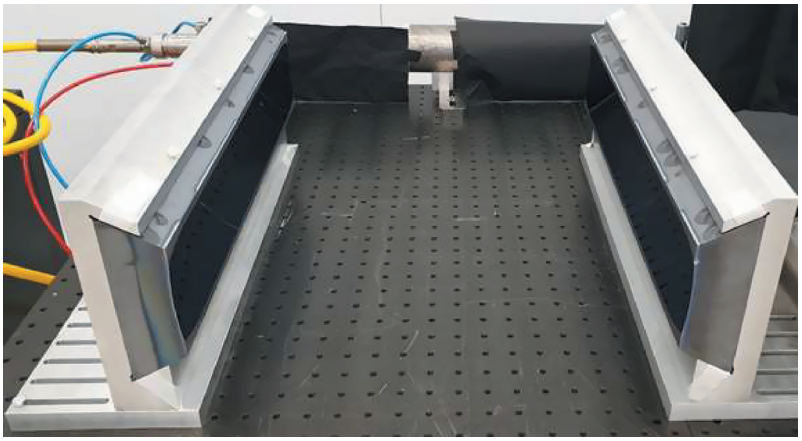

Fig. 14. Photon accumulator in the study of the efficiency of the accumulation of radiant energy.

(i) Measurement of the negative ion current during the modulation of the laser radiation;

(ii) Recording the dependence of the neutralization degree on the beam particle energy and on the pumping power;

(iii) Reaching the maximum possible neutralization in the quasi-stationary regime;

(iv) Development of the system of mirror cooling and transition to the stationary operation regime;

(v) Measuring the mean operating time between failures.

Given the simple dependence (1), the first two stages will allow us to verify the operability and veracity of the concept of nonresonant accumulation. If the result of the third stage agrees with the calculations (neutralization exceeds 70% at an energy of 100 keV), this will demonstrate the possibility of creating mirrors of a complicated shape and high reflectivity that are sufficiently resistant to high flows of radiant energy per unit surface. The fourth stage will allow us to find the most optimum ways of effectively cooling the mirrors, which is a substantial problem in larger systems. The fifth stage will determine the approximate lifetime of the neutralizer. Probably, it will be limited by the destruction of the coating under the bombarding of the scattered high-energy particles. Since the physics of such scattering is based on pair collisions, the obtained results can be recalculated for large installations such as TRT and ITER.

The success of the proposed photon neutralization concept according to [6] will allow us to increase the commercial attractiveness of the thermonuclear power industry.

7. CONCLUSIONS

The nonresonant accumulation of radiation for the photoneutralization of the negative ions in the systems with neutral injection has an undeniable advantage compared to the resonant accumulation due to the commercial availability of high-energy radiation sources. These sources have sufficient radiation quality and a high efficiency of up to 45% [14]. Despite the substantial power and the expenses for the generation of radiation (see Table 1), one can expect that the total efficiency of the heating systems will increase, at minimum, two times. When the output current of atoms is decreased, the efficiency can increase even more due to the simplification of the accelerator part of the injector and the connected increase in its efficiency. For a better and more efficient cooping of the width of the region occupied by the photons and the beam cross section, the most convenient shape is elongated in one direction.

The main obstacle to the effective neutralization is the production of large mirrors with a high total efficiency of the mirror surface. Also of principal importance is the longevity of the mirror surface.

Thus, the experiment that is carried out at BINP SB RAS will answer the question of the exploitability of the nonresonant photon target for neutralization.

FUNDING

This work was supported by the Ministry of Science and Higher Education of the Russian Federation.

CONFLICT OF INTEREST

The authors of this work declare that they have no conflicts of interest.

REFERENCES

1. R. Hemsworth, H. Decamps, J. Graceffa, B. Schunke, M. Tanaka, M. Dremel, A. Tanga, H. P. L. De Esch, F. Geli, J. Milnes, T. Inoue, D. Marcuzzi, P. Sonato, and P. Zaccaria, Nucl. Fusion **49**, 045006 (2009). https://doi.org/10.1088/0029-5515/49/4/045006
2. G. I. Dimov and G. V. Roslyakov, Nucl. Fusion **15**, 551 (1975). https://doi.org/10.1088/0029-5515/15/3/021
3. L. M. Branscomb and S. J. Smith, Phys. Rev. Lett. **98**, 1028 (1955).
4. S. J. Smith and D. S. Burch, Phys. Rev. Lett. **2**, 165 (1959).
5. A. M. Frolov, J. Phys. B: At., Mol. Opt. Phys. **37**, 853 (2004).
6. R. S. Hemsworth and D. Boilson, AIP Conf. Proc. **1869**, 060001 (2017). https://doi.org/10.1063/1.4995788
7. J. H. Fink and A. M. Frank, Technical Report No. UCRL-16844 (Lawrence Livermore National Laboratory, Livermore, CA, 1975).
8. V. Vanek, T. Hursman, D. Copeland, and D. Goebel, in *Proceedings of the 3rd International Symposium on Production and Neutralization of Negative Ions and Beams, Brookhaven, NY, 1983*, p. 568.
9. W. Chaibi, C. Blondel, L. Cabaret, C. Delsart, C. Drag, and A. Simonin, AIP Conf. Proc. **1097**, 385 (2009).
10. M. Kovari and B. Crowley, Fusion Eng. Des. **85**, 745 (2010).
11. A. Simonin, Jocelyn Achard, K. Achkasov, S. Bechu, C. Baudouin, O. Baulaigue, C. Blondel, J. P. Boeuf, D. Bresteau, G. Cartry, W. Chaibi, C. Drag, H. P. L. de Esch, D. Fiorucci, G. Fubiani, et al., Nucl. Fusion **55**, 123020 (2015). https://doi.org/10.1088/0029-5515/55/12/123020
12. D. Fiorucci, J. Feng, M. Pichot, and W. Chaibi, AIP Conf. Proc. **1655**, 050010 (2015). https://doi.org/10.1063/1.4916467
13. D. Fiorucci and A. Fassina, Eur. Phys. J. D **76**, 141 (2022). https://doi.org/10.1140/epjd/s10053-022-00457-9
14. IPG Photonics Corporation, Lasers of YLS series. https://www.ipgphotonics.com/ru/products/lasers/nepreryvnye-lazery-vysokoy-moshchnosti. Cited October 25, 2023.
15. S. S. Popov, M. G. Atlukhanov, A. V. Burdakov, and M. Yu. Ushkova, Opt. Spectrosc. **121**, 160 (2016). https://doi.org/10.1134/S0030400X16070183
16. S. S. Popov, M. G. Atlukhanov, A. V. Burdakov, and M. Yu. Ushkova, Laser Phys. **28**, 096201 (2018). https://doi.org/10.1088/1555-6611/aacb54
17. S. S. Popov, M. G. Atlukhanov, A. V. Burdakov, A. A. Ivanov, A. A. Kasatov, A. V. Kolmogorov, R. V. Vakhrushev, M. Yu. Ushkova, A. Smirnov, and A. Dunaevsky, Nucl. Fusion **58**, 096016 (2018). https://doi.org/10.1088/1741-4326/aacb02
18. S. S. Popov, M. G. Atlukhanov, A. V. Burdakov, A. A. Ivanov, A. V. Kolmogorov, M. Yu. Ushkova, and R. V. Vakhrushev, AIP Conf. Proc. **2011**, 060005 (2018). https://doi.org/10.1063/1.5053334
19. Yu. I. Belchenko, A. V. Burdakov, V. I. Davydenko, A. I. Gorbovskii, I. S. Emelev, A. A. Ivanov, A. L. Sanin, and O. Z. Sotnikov, Plasma Phys. Rep. **47**, 1151 (2021). https://doi.org/10.1134/S1063780X21110131
20. Yu. I. Belchenko, V. I. Davydenko, G. E. Derevyankin, G. I. Dimov, V. G. Dudnikov, I. I. Morosov, G. V. Roslyakov, and A. L. Schabalin, Rev. Sci. Instrum. **61**, 378 (1990). https://doi.org/10.1063/1.1141299
21. A. Sanin, Yu. Belchenko, A. Ivanov, and A. Gmyrya, Rev. Sci. Instrum. **90**, 123314 (2019). https://doi.org/10.1063/1.5128590

Translated by E. Voronova